JOURNAL OF CATALYSIS 150, 81–93 (1994)

Infrared Studies of the Mechanism of Methanol Decomposition on Cu/SiO_2

Dean B. Clarke, Dong-Keun Lee, Mark J. Sandoval, and Alexis T. Bell

Chemical Sciences Division, Lawrence Berkeley Laboratory, Berkeley, California 94720; and Department of Chemical Engineering, University of California, Berkeley, California 94720-1462

Received February 11, 1994; revised June 27, 1994

The mechanism of methanol decomposition on silica-supported Cu has been investigated by means of infrared spectroscopy and temperature-programmed desorption spectroscopy. Infrared spectra taken during both isothermal and temperature-programmed experiments reveal the following species: methanol, methoxy groups, formaldehyde, methylenebis(oxy) groups, and formate groups. The only products observed during temperature-programmed decomposition are formaldehyde, carbon dioxide, hydrogen, and water. The ratio of hydrogen to carbon dioxide is 0.5 indicating that both products are formed by the decomposition of formate groups on the surface of copper. A mechanism for methanol decomposition is proposed, based on the sequence of species observed during temperature-programmed infrared (TPD-IR) experiments. Simulations of the TPD-IR experiments based on the proposed scheme provide an accurate representation of the observed variations in the concentrations of adsorbed species.

INTRODUCTION

The pathway for methanol decomposition over Cu is closely related to the pathway for methanol synthesis and, hence, much can be learned about the mechanism of methanol synthesis by studying its decomposition. Investigations of methanol adsorption and decomposition on reduced and oxidized Cu(100) and (110) surfaces have shown that CH_3OH readily undergoes dissociative adsorption to form CH_3O_s species (1–7). The presence of preadsorbed oxygen enhances the formation of CH_3O_s species and stabilizes them to further decomposition. On reduced Cu surfaces, CH_3O_s species decompose near 370 K to form formaldehyde and methyl formate. When preadsorbed oxygen is present, part of the CH_3O_s species react to form $HCOO_s$ groups. These latter species decompose around 400 K to produce CO_2 and H_2. Recent studies of methanol chemisorption on Cu/SiO_2 have given a similar picture of the sequence of steps involved in methanol decomposition (8, 9). While adsorbed formaldehyde, CH_2O_s, and methylenebis(oxy) (known alternatively as dioxymethylene), $CH_2(O)_{2,s}$, have been proposed as intermediates in the decomposition of adsorbed methanol on Cu, no direct evidence for these species has been presented (1, 8).

The present investigation was undertaken to obtain a more detailed picture of the mechanism and dynamics of methanol decomposition over silica-supported Cu. *In situ* infrared spectroscopy was used to observe the structure and surface concentration of adsorbed species during the exposure of a Cu/SiO_2 catalyst at room temperature and during the temperature-programmed decomposition of adsorbed methanol. Complementary TPD studies were conducted to identify the gas-phase products produced during methanol decomposition. The results of this work show that it is possible to observe the principal intermediates involved in the decomposition of methanol on Cu and to determine the activation energies for some of the elementary processes.

EXPERIMENTAL

A 7% Cu/SiO_2 catalyst was prepared by ion exchange on Cab-O-Sil M5 following the procedures described in Ref. (10). The BET surface area of the catalyst is 203 m^2/g and the Cu surface area measured by CO chemisorption (11) is 18.2 m^2/g, which corresponds to a Cu dispersion of 38%. About 50 mg of the catalyst was pressed into a 2-cm diameter disk and placed inside a low dead volume (0.4 cm^3) infrared cell (12). The catalyst was reduced in H_2 for 3 h or more at 513 K. For the experiment performed on a preoxidized sample, the catalyst was heated in 1 atm of O_2 at 363 K for 1.5 h. These conditions were chosen to avoid bulk oxidation of Cu which can occur at temperatures above 378 K (13). Methanol adsorption onto the catalyst was from an UHP argon (99.999% pure) stream containing 0.99% of methanol. The stainless-steel tubing leading up to the infrared cell was heat to 373 K to avoid methanol condensation.

Infrared spectra were recorded with a Digilab FTS-80 FTIR spectrometer operated with a resolution of 2–4

0021-9517/94 $6.00

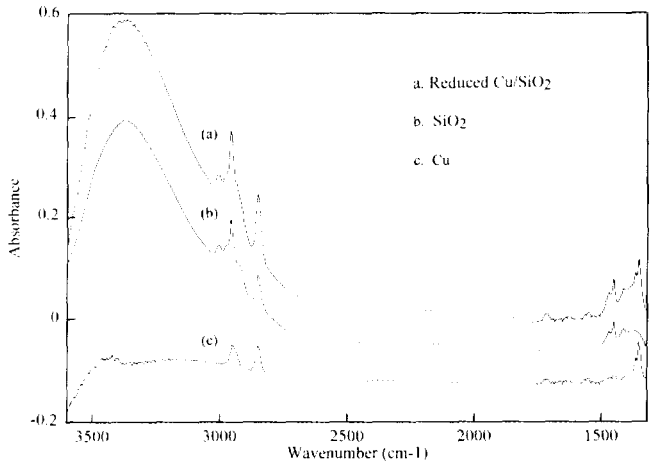

FIG. 1. Infrared spectra of methanol adsorbed on (a) reduced Cu/SiO_2, (b) SiO_2, and reduced Cu following exposure to 0.1% methanol in Ar for 30 min. Spectrum (c) = spectrum (a) − 1.2 × spectrum (b).

cm^{-1}. To achieve satisfactory signal-to-noise ratio, 64–256 scans were averaged. A typical spectrum based on 64 scans at 4 cm^{-1} resolution was acquired in about 30 s. After acquisition, spectra were deconvolved into their components by using a least-squares regression curve fitting routine called GRAMS 486 (Galactic Industries Corp.) run on a 486 PC.

Complementary temperature-programmed desorption (TPD) studies were carried out with an 8.7% Cu/SiO_2 catalyst prepared in a manner similar to that described above for the 7% Cu/SiO_2 catalyst used for the infrared studies. The dispersion of the 8.7% Cu/SiO_2 catalyst is 18%. TPD experiments were carried out by using the apparatus described in Ref. (14), which consists of a quartz microreactor connected upstream to a gas handling manifold and downstream to a mass spectrometer (UTI Model 100C). Calibration of the mass spectrometer enabled quantitative analyses to be made of the desorption products. Approximately 0.1 g of the 8.7% Cu/SiO_2 catalyst was used for the TPD experiments.

RESULTS

Figure 1 shows infrared spectra taken after exposure of reduced Cu/SiO_2 (spectrum a) and SiO_2 (spectrum b) to a 0.1% methanol in Ar stream for 30 min at 303 K. To obtain the spectrum of methanol adsorbed on Cu alone, spectrum b was subtracted from spectrum a. The result is shown as spectrum c. Spectra a and b exhibit a broad band centered around 3400 cm^{-1} characteristic of OH stretching vibrations, and all three spectra exhibit bands between 3100 and 2800 cm^{-1} characteristic of C–H stretching vibrations and bands below 1800 cm^{-1} characteristic of C–H bending and C–O stretching modes. A comparison of the spectrum for methanol adsorbed on reduced and oxidized Cu/SiO_2 is shown in Fig. 2. (For this and all subsequent experiments the adsorption of methanol was from a 1% methanol in Ar stream at 303 K.) While the features appearing in the region of 3100–2800 cm^{-1} are qualitatively similar for reduced and oxidized Cu, noticeable differences are evident in the portions of the spectra appearing below 1800 cm^{-1}.

To facilitate the determination of band positions and intensities, the spectra presented in Figs. 1 and 2 were deconvolved. The results of this procedure are shown in Figs. 3–5 for the spectral regions of 3100–2800 and 1550–1300 cm^{-1}. For methanol adsorption on SiO_2, Fig. 3 shows well defined bands at 3003, 2977, 2921, 2956, 2848, 1470, 1451, 1415, and 1366 cm^{-1}. The spectrum of methanol adsorbed on reduced Cu shown in Fig. 4 exhibits bands at 2951, 2935, 2851, 1722, 1713, 1564, 1553, 1450, 1388, 1366, and 1351 cm^{-1}, whereas the spectrum of methanol adsorbed on oxidized Cu, shown Fig. 5, shows bands at 2994, 2953, 2920, 2850, 2824, 2765, 1722, 1712, 1592, 1467, 1450, and 1405 cm^{-1}.

Assignments of the features appearing in Figs. 1–5 were made by analogy with the spectra of known compounds and by comparison with previous studies of a similar nature. The results of this exercise are presented in Table 1 for SiO_2 and in Tables 2 and 3 for reduced and oxidized Cu, respectively. Listed in each of these tables are the species and vibrational mode associated with each of the bands observed in this study, the positions of similar bands reported in previous studies of CH_3OH adsorbed on SiO_2 and Cu/SiO_2, and the positions of bands for gas-phase adsorbates or for model systems such as organometallic complexes or CH_3OH adsorbed on Cu single crystals.

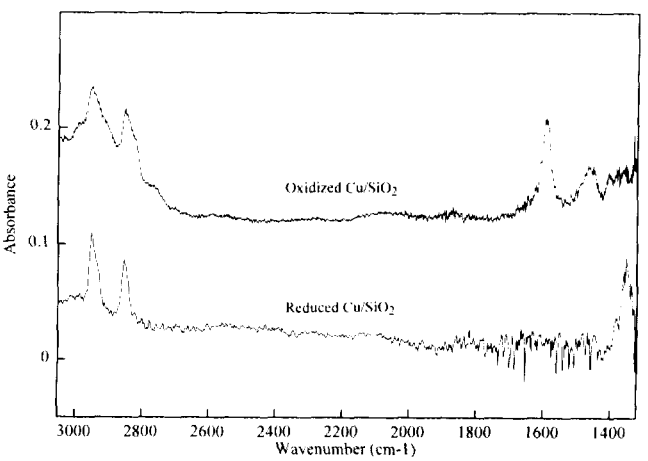

FIG. 2. Infrared spectra of methanol adsorbed on (top) oxidized and (bottom) reduced Cu/SiO_2 following exposure at 303 K to 1% methanol in Ar for 60 min and subsequent purging in Ar for 30 min. The spectrum of SiO_2 in Ar at 303 K has been subtracted from each spectrum.

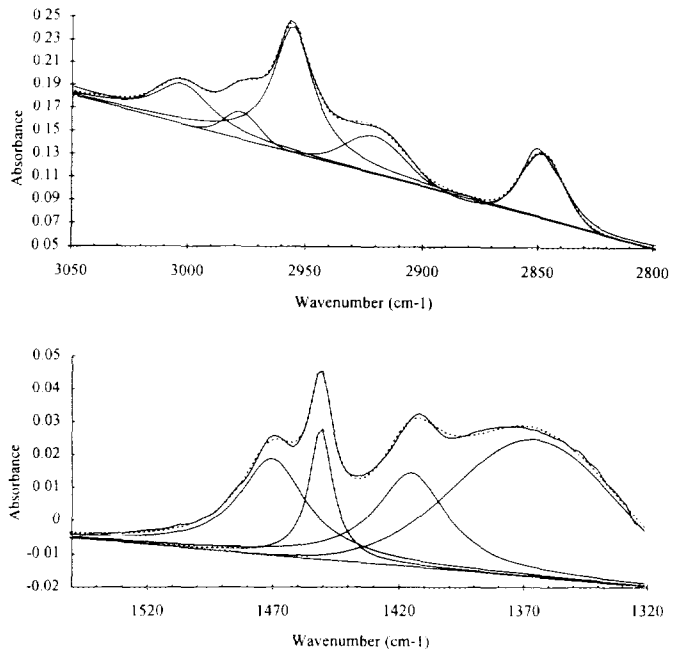

FIG. 3. Deconvolution of spectrum (b) in Fig. 1 for methanol adsorbed on SiO_2.

All of the features in the spectrum of CH_3OH adsorbed on SiO_2 can be ascribe to physisorbed CH_3OH. The broad band at 3370 cm^{-1} in the spectrum of methanol adsorbed on SiO_2 is attributable to O–H vibrations in CH_3OH hydrogen-bonded to SiOH groups (15). As the intensity of this band increases, the band at 3744 cm^{-1} for isolated Si–OH groups on the silica surface (not shown) decreases in intensity as a consequence of hydrogen bonding between the physisorbed CH_3OH and the Si–OH groups. The bands located at 3003, 2956, and 2848 cm^{-1} can be ascribed to C–H bond vibrations in weakly adsorbed CH_3OH (8, 16), whereas the bands at 1470 and 1451 cm^{-1} are due to CH_3 bending vibrations (8, 16). The appearance of three C–H stretching vibrations is indicative of the unsymmetric structure of physisorbed CH_3OH. The band at 1377 cm^{-1} is due to in-plane bending vibrations of OH groups (8, 17). In agreement with previous studies, the band at 2921 cm^{-1} is ascribed to an overtone of one of the CH_3 bending modes (8, 16).

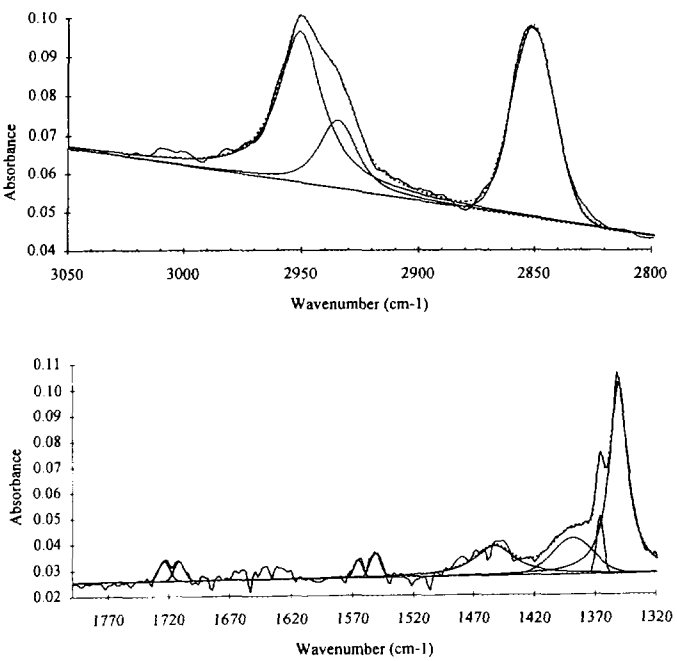

FIG. 4. Deconvolution of spectrum (c) in Fig. 1 for methanol adsorbed on reduced Cu/SiO_2.

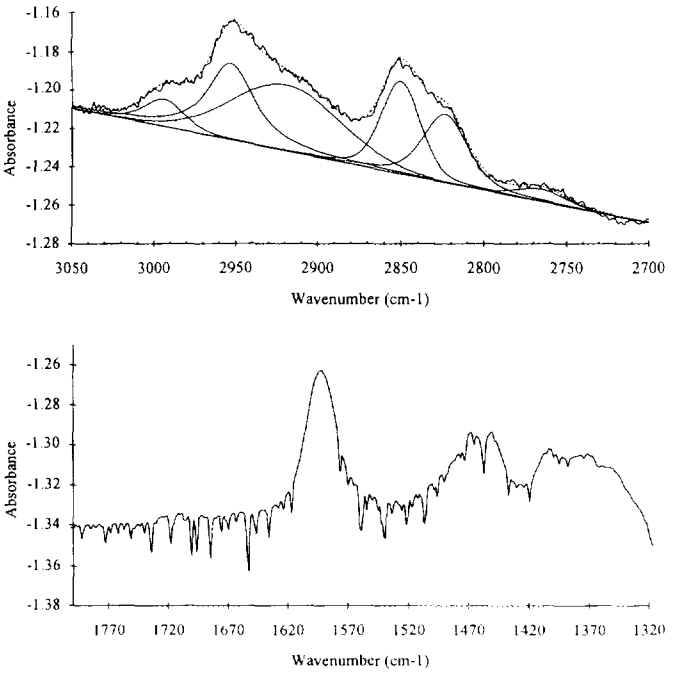

FIG. 5. Deconvolution of the spectrum shown in Fig. 2 for oxidized Cu/SiO_2. The portion of the spectrum between 1820–1320 cm^{-1} has not been corrected by subtraction of a SiO_2 reference spectrum. Since the peaks appearing in this region are well resolved, the peak deconvolution program was not run for this portion of the spectrum.

The band at 2977 cm^{-1} is not readily assigned. Morrow (16) has reported a band at 2974 cm^{-1} for methoxy groups on silica produced by methoxylation of silica at 673 K and attributed this band to C–H vibrations in a symmetric $Si–OCH_3$ species. However, the assignment of the band at 2977 cm^{-1} to methoxy groups does not seem appropriate for the conditions of the present study. As reported by Borrello *et al.* (15), the formation of methoxy groups during room temperature exposure of silica occurs only on silica that has previously been heated in vacuum or in an inert atmosphere above 623 K to produce strained

TABLE 1

Assignments of Infrared Bands Observed for CH_3OH Adsorbed at 303 K on SiO_2

Species	Mode	This study (cm^{-1})	Prev. studies (cm^{-1})	Model systems (cm^{-1})
CH_3OH	ν_{OH}	3370	3370 (15)	—
CH_3OH	ν_{CH}	3003	3000 (8, 16)	3000 for CH_3 in a Sn complex (19)
CH_3OH	ν_{CH}	2977	2974 (16)	2982 for CH_3OH_g (20)
CH_3OH	ν_{CH}	2956	2958 (16); 2955 (8); 2950 (15)	—
CH_3OH	ν_{CH}	2921	2931 (8); 2928 (16)	—
CH_3OH	ν_{CH}	2848	2858 (16); 2845 (1, 15)	2845 for CH_3OH_g (20)
CH_3OH	δ_{CH}	1470	1467 (8)	1473 for CH_3O in a Ga complex (21); 1458 for CH_3 in a Sn complex (19)
CH_3OH	δ_{CH}	1451	1464 (16)	1455 for CH_3OH_g (20)
CH_3OH	δ_{OH}	1366	1371 (8, 17)	1346 for CH_3OH_g (20)

Si–O–Si bonds. While the formation of $Si–OCH_3$ groups could also occur via condensation of CH_3OH with Si–OH groups, Sidorov (18) has shown that this reaction does not occur at temperatures below 673 K. Since the silica used for the present experiments was never heated in Ar or H_2 above 569 K and methanol exposure occurred only at room temperature, it is unlikely that methoxy groups were formed upon exposure of the silica to methanol. Further supporting this conclusion is the observation, reported below, that most of the adsorbed methanol is desorbed upon flushing in Ar at room temperature and the small residuum is removed by heating to 400 K. Morrow (16), on the other hand, has reported that $Si–OCH_3$ groups are stable up to 723 K. Thus, while not due to methoxy groups, the band at 2977 cm^{-1} could conceivable be ascribed to C–H stretching vibrations of symmetrically physisorbed CH_3OH.

The spectrum of CH_3OH adsorbed on SiO_2 also contains a band at 1415 cm^{-1}. This feature is best assigned to vibrations of a carbonate group (22); however, the

TABLE 2

Assignments of Infrared Bands Observed for CH_3OH Adsorbed at 303 K on Reduced Cu/SiO_2

Species	Mode	This study (cm^{-1})	Prev. studies (cm^{-1})	Model systems (cm^{-1})
CH_3OH	ν_{CH}	2951	2955 (8)	—
CH_3OH	ν_{CH}	2851	2845, 2841 (8)	2845 for CH_3OH_g (20)
CH_3OH	δ_{OH}	1388	—	1346 for CH_3OH_g (20)
CH_3O	ν_{CH}	2888[c]	2890 (8)	2887 for CH_3O in an Os complex (26); 2882 for CH_3O on Cu(111) (27)
CH_3O	ν_{CH}	2822[c]	2815 (8)	2836, 2828 for CH_3O in a Ga complex (21); 2822 for CH_3O in an Os complex (26); 2830 for CH_3O on Cu(100) (28)
CH_2O	ν_{CO}	1713, 1722	1727 (23)	1742 for CH_2O_g (20)
m-HCOO[a]	ν_{CH}	2902[c]	2904 (24)	2891-2900 for *m*-HCOO on Cu(110) (20)
m-HCOO	ν_{COO}	1564[d]	1583 (25); 1574 (8, 24)	1585 for *m*-HCOO in a Re complex (30)
m-HCOO	ν_{COO}	1366	1360 (25); 1359 (24)	1371 for *m*-HCOO on oxidized Cu film (30)
b-HCOO[b]	ν_{COO} + δ_{OH}	2935	2938 (25); 2937 (24)	2950 for *b*-HCOO on Cu(110) (32, 33)
b-HCOO	ν_{CH}	2851	2845, 2841 (8)	2841 for HCOONa (34)
b-HCOO	ν_{COO}	1553	1557 (8); 1552 (25)	1560 for *b*-HCOO on Cu(110) (28)
b-HCOO	ν_{COO}	1351	1359 (24); 1352 (8); 1350 (25)	1358 for *b*-HCOO on Cu(110) (28, 29)

[a] Monodetate formate.
[b] Bidentate formate.
[c] Observed only at elevated temperatures.
[d] Observed only at room temperature.

TABLE 3

Assignments of Infrared Bands Observed for CH_3OH Adsorbed at 303 K on Oxidized Cu/SiO_2

Species	Mode	This study (cm^{-1})	Prev. studies (cm^{-1})	Model systems (cm^{-1})
CH_3OH	ν_{CH}	2994	—	3000 for CH_3 in a Sn complex (19)
CH_3OH	ν_{CH}	2953	2955 (8)	—
CH_3OH	ν_{CH}	2850	2845, 2841 (8)	2845 for CH_3OH_g (20)
CH_3OH	δ_{CH}	1451	—	1455 for CH_3OH_g (20)
CH_3O	ν_{CH}	2920	2926 (8)	2920 for CH3O in a Re complex (35); 2910 for CH_3O on Cu(100) (27)
CH_3O	ν_{CH}	2880[b]	2890 (8)	2882 for CH_3O on Cu(111) (28)
CH_3O	ν_{CH}	2824	2815 (8)	2822 for CH_3O in an Os complex (26)
CH_2O	ν_{CO}	1713, 1722	1727 (23)	1742 for CH_2O_g (20); 1740 for CH_2O on Cu(110) (32)
$CH_2(O)_2$	ν_{CH}	2765	—	2763 for anatase (36); 2750 for thoria (36)
$CH_2(O)_2$	δ_{CH}	1405	—	1408 for anatase (36)
m-HCOO[a]	ν_{CH}	2902	2904 (24)	2891–2900 for *m*-HCOO on Cu(110) (29)
m-HCOO	ν_{COO}	1592	1583 (25); 1574 (8, 24)	1585 for *m*-HCOO in a Re complex (30)
m-HCOO	ν_{COO}	1366	1360 (25); 1359 (24)	1371 for *m*-HCOO on oxidized Cu film (31)
H_2O	δ_{OH}	1626	1630 (8)	1635 for H_2O_g (20)

[a] Monodentate formate.
[b] Observed only at elevated temperatures.

origin of this species cannot be explained since, as discussed below, CH_3OH does not decompose over pure SiO_2. Conceivably, this band might be attributable to small quantities of sodium carbonate associated with the very small Na impurity in the silica; however, the Na content determined by X-ray flouresence is only 1.1 ppm.

As shown in Tables 2 and 3, the features observed upon room-temperature adsorption of methanol on reduced and oxidized Cu can be ascribed to a variety of species. On reduced Cu adsorbed CH_3OH is characterized by C–H stretching vibrations at 2951 and 2851 cm^{-1} and an OH bending vibration at 1388 cm^{-1} (8, 20). The band at 1388 cm^{-1} is not observed on oxidized Cu but an additional C–H stretching vibration is seen at 2994 cm^{-1}. The presence of CH_3O groups on oxidized Cu is evidenced by C–H stretching vibrations appearing at 2920 and 2824 cm^{-1} (5, 8, 26–27). When methanol is adsorbed on oxidized Cu at elevated temperatures an additional C–H stretching band is observed at 2880 cm^{-1}. Bands at 2880 and 2824 cm^{-1} are also observed on reduced Cu when methanol is adsorbed on both reduced and oxidized Cu at elevated temperatures. Adsorbed CH_2O is observed on both reduced and oxidized Cu, as characterized by C–O stretching bands appearing at 1722 and 1713 cm^{-1} (20, 23). Bands appearing at 2765 and 1405 cm^{-1} in the spectra of methanol adsorbed on reduced and oxidized Cu are assigned to methylenebis(oxy), $CH_2(O)_2$, groups based on the work of Lavalley *et al.* (36), who observed similar features upon room-temperature adsorption of CH_2O on thoria and titania. Predominantly bidentate formate groups were observed on reduced Cu, although bands characteristic of monodentate formate groups were also detectable under special circumstances as noted in Table 2. On oxidized Cu only monodentate formate groups were detected. The bands observed on reduced Cu at 2902, 1564, and 1366 cm^{-1} are assigned to monodentate formate groups, *m*-HCOO, (8, 24, 25, 29–31), whereas the bands at 2935, 2851, 1553, and 1351 cm^{-1} are assigned to bidentate formate groups, *b*-HCOO, (8, 24, 25, 28, 29, 32–34).

The extinction coefficients for methanol adsorbed on SiO_2 and reduced Cu were determined in the following fashion. The adsorption isotherm for methanol at 303 K was measured by volumetric uptake for methanol partial pressures of 6×10^{-3} to 5.4 Torr. Over this range of pressures, the methanol uptake on SiO_2 and Cu/SiO_2 was identical. In both cases the adsorption of methanol was totally reversible and obeyed a Henry's law with a Henry's law constant of 3.7×10^{-2} μmol/(g Torr). The fractional coverage of methanol on Cu was calculated by assuming a partitioning of the adsorbed methanol between Cu and SiO_2 in proportion to their surface areas. Figure 6 shows the relation of the peak intensity of the C–H stretching mode of methanol occurring at 2953 cm^{-1} to the fractional coverage of the Cu surface. The extinction coefficient determined from the slope of this curve decreases with coverage in a manner similar to that observed

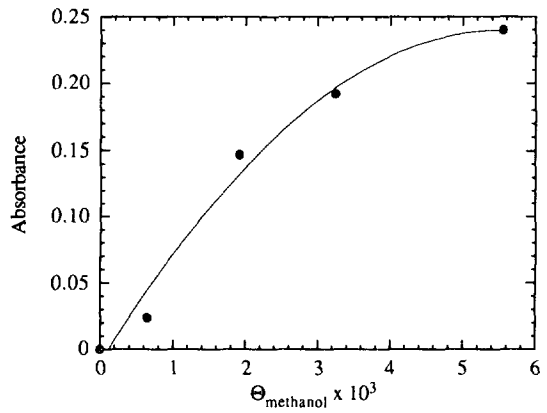

FIG. 6. Variation in the absorbance of the band at 2953 cm^{-1} with coverage for methanol adsorbed on reduced Cu.

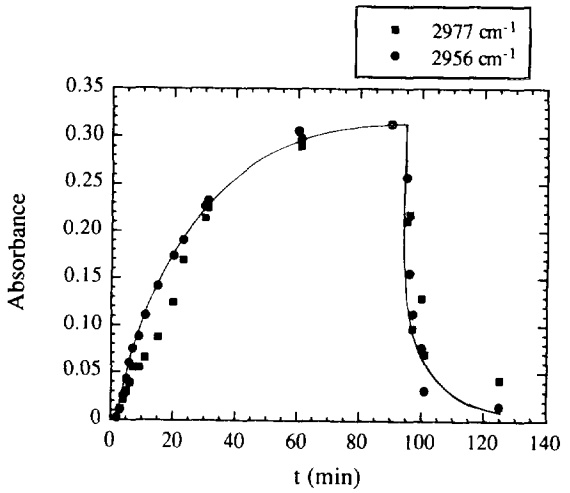

FIG. 7. Temporal dependence of the bands assigned to CH_3OH appearing at 2977 and 2953 cm^{-1} during the exposure of SiO_2 to 1% methanol in Ar at 303 K and subsequent purging in Ar starting at 95 min.

for the adsorption of CO on Ru (37). The extinction coefficient for methanol adsorbed on Cu is reported in Table 4, based on both the integrated peak area and the peak intensity. Extinction coefficients are also reported in Table 4 for methanol adsorption on SiO_2. The values of the extinction coefficients for methanol adsorbed on Cu and SiO_2 are comparable to those reported previously for CO adsorbed on Cu (10, 38).

Observations were made of the temporal evolution of the spectrum upon exposure of SiO_2 and both reduced and oxidized Cu/SiO_2 to a flowing stream of Ar containing 1% methanol at 303 K. When the intensities of the observed features approached steady-state values, the flow of Ar containing methanol was switched to a flow of pure Ar. Plots of the intensities of specific adsorbed species versus time are shown in Figs. 7–9.

It is apparent from Fig. 7 that the intensities of the bands at 2956 and 2977 cm^{-1} track each other vary closely during both the adsorption and desorption phases of the experiment. This pattern supports the assignment of the band at 2977 cm^{-1} to physisorbed CH_3OH, as noted above.

TABLE 4

Infrared Extinction Coefficients for Methanol Based on the C–H Band at 2953 cm^{-1}

Surface	CH_3OH Ads. (μmol/g)	ε based on peak height (cm^2/molecule)	ε based on peak area ($cm^{-1} \cdot cm^2$/molecule)
SiO_2	5	2.4×10^{-18}	2.4×10^{-17}
	25	5.0×10^{-19}	2.4×10^{-17}
Cu	0.5	1.6×10^{-17}	1.9×10^{-16}
	2	4.3×10^{-18}	4.7×10^{-17}

Figure 8 shows that in contrast to the case of SiO_2, methanol adsorption on reduced Cu is very rapid but passes through a maximum after 20 min of exposure. No evidence for methoxy species can be observed, but bands are seen to build up for both adsorbed formaldehyde and bidentate formate, during the period of methanol exposure. Because the signal-to-noise ratio for the spectra presented in Fig. 8 is lower than that for the spectra presented in Fig. 1, bands for monodentate formate species could not be detected. When the flow of methanol is terminated, Fig. 8 shows that the intensities of the bands for formaldehyde and bidentate formate species decrease only slightly. The pattern for oxidized Cu is similar to that for reduced Cu. Figure 9 shows a rapid build up in

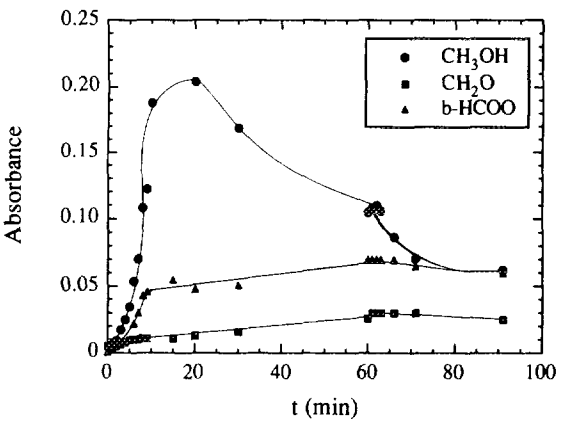

FIG. 8. Temporal dependence of the bands assigned to CH_3OH (2951 cm^{-1}), CH_2O (1727 cm^{-1}), and bidentate HCOO (1351 cm^{-1}) during the exposure of reduced Cu/SiO_2 to 1% methanol in Ar at 303 K and subsequent purging in Ar starting at 61 min.

the intensity of the feature attributed to methanol and a slower increase in the intensity of the band associated with formate species. In contrast to what is observed for reduced Cu, noticeable quantities of methoxy species are observed and the intensity of the band attributed to formaldehyde is initially much more intense. The surface concentration of formaldehyde rises very rapidly, passes through a maximum, and then decrease with increasing length of methanol exposure. It is noted as well that on oxidized Cu the presence of methylenebis(oxy) species can be observed during the purge of the infrared cell with Ar.

The desorption and surface reaction of strongly adsorbed species present on the surface of SiO_2 and Cu/SiO_2 were observed by recording a series of infrared spectra at 1 min intervals while heating the catalyst at 5 K/min. Figure 10 illustrates the TPD-IR spectra for methanol adsorbed at 303 K on SiO_2 that had been heated at 513 K for 3 h in flowing H_2. Each of the spectra shown was deconvolved so that a plot of band adsorbance versus temperature could be produced. Figure 11 shows a plot of the absorbance for adsorbed methanol. Using the methanol extinction coefficient presented in Table 3, it is estimated that the surface coverage by methanol at the beginning of the temperature ramp is 2×10^{-5} ml. Figures 10 and 11 show that most of the adsorbed species have disappeared by 350 K and that the remainder of the species leave the surface by desorption and reaction more slowly as the temperature is raised to 450 K.

TPD-IR spectra for methanol adsorbed on reduced Cu/SiO_2 are presented in Fig. 12. Deconvolution of these spectra and subtraction of the corresponding spectra for methanol adsorbed on SiO_2 enables the determination of the intensities of the features for species adsorbed exclusively on reduced Cu. A plot of the fractional coverages for methanol, formaldehyde, methoxy species and bidentate formate species in presented in Fig. 13. The initial coverage of methanol is 1×10^{-3} ML. It is evident from Fig. 13 that the surface concentration of methanol adsorbed on Cu falls almost to zero by the time the temperature reaches 400 K. The concentration of adsorbed formaldehyde decreases very rapidly, approaching zero at 350 K. A very small amount of methoxy species is observed in the temperature interval of roughly 350–360 K. The surface concentration of bidentate formate species rises to a maximum at 400 K and then decreases monotonically, approaching zero at about 500 K. Monodentate formate species disappeared at room temperature upon purging and were absent throughout the period of temperature-programmed desorption.

Figure 14 shows TPD-IR spectra for methanol adsorbed on oxidized Cu/SiO_2. In the course of these experiments, two bands were observed very clearly for methylenebis(oxy) at 2765 and 1404 cm^{-1}, as can be seen in Fig.

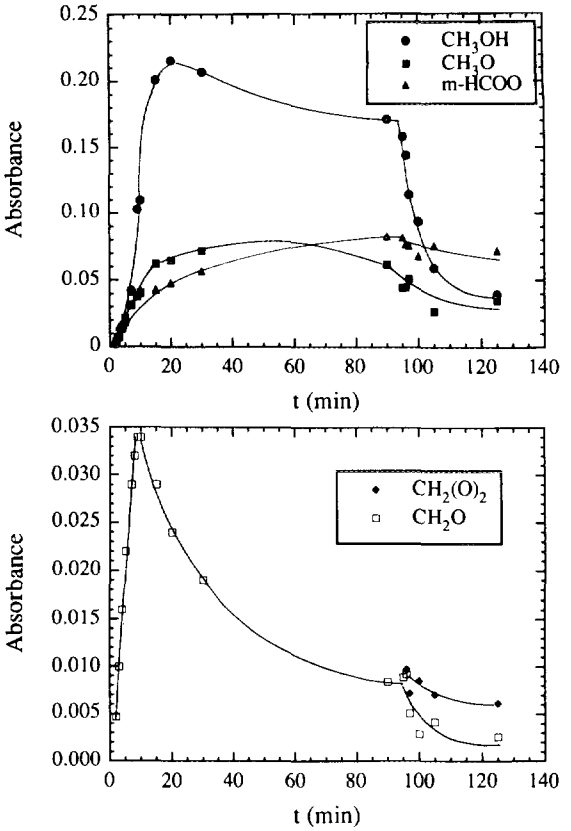

FIG. 9. Temporal dependence of the bands assigned to CH_3OH (2953 cm^{-1}, CH_3O (2824 cm^{-1}), CH_2O (1727 cm^{-1}), $CH_2(O)_2$ (2765 cm^{-1}), and monodentate HCOO (1592 cm^{-1}) during the exposure of oxidized Cu/SiO_2 to 1% methanol in Ar at 303 K and subsequent purging in Ar starting at 95 min.

15. The variation with temperature in the intensity of individual species adsorbed on the oxidized Cu surface was obtained in the same manner as described above for reduced Cu. Figure 16 shows plots of the variation in absorbance with temperature for the bands associated with adsorbed methanol and formaldehyde, as well as the bands associated with methoxy, methylenebis(oxy), and monodentate formate species. The intensity of the methoxy band passed through a local maximum between 340 and 350 K, which coincides with the temperature range where this band is detectable on reduced Cu. On reduced Cu, the monodentate formate species were stable to higher temperatures than the bidentate formate species, and decomposed only above 465 K.

Attempts to analyze the composition of the effluent gases during the temperature-programmed infrared experiments proved to be impractical because of the small amount of catalyst used and the slow heating rate, both of which resulted in very low concentrations of the desorbing species in the gas phase. As a consequence, TPD experi-

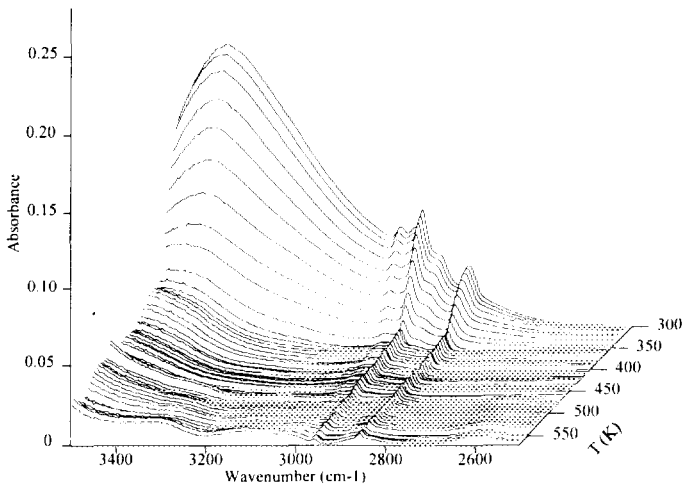

FIG. 10. Infrared spectra obtained during temperature-programmed desorption of methanol from SiO_2. SiO_2 is first exposed to 1% methanol in Ar at 303 for 10 min, purged in Ar at 303 K for 26 min, and then continuously purged in Ar as the temperature is increased at 5 K/min from 303 to 568 K. Spectra are recorded at 1 min intervals. The spectrum of pure SiO_2 recorded at the same temperature in Ar has been subtracted from each spectrum.

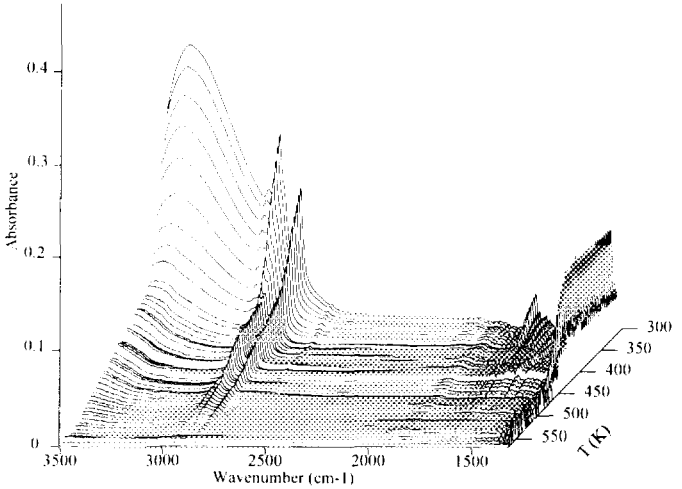

FIG. 12. Infrared spectra obtained during temperature-programmed desorption of methanol from reduced Cu/SiO_2. Cu/SiO_2 is first exposed to 1% methanol in Ar at 303 K for 10 min, purged in Ar at 303 K for 26 min, and then continuously purged in Ar as the temperature is increased at 5 K/min from 303 to 568 K. Spectra are recorded at 1 min intervals. The spectrum of reduced Cu/SiO_2 recorded at the same temperature in Ar has been subtracted from each spectrum.

ments were carried out separately on SiO_2 and an 8.7% Cu/SiO_2 catalyst.

Figure 17 shows the TPD spectrum for methanol adsorbed on SiO_2 at 298 K for 5 min from a stream containing 1% methanol in He. A heating rate of 10 K/min and He a flowrate of 20 cm^3/min were used for the TPD experiment. The principal feature in the spectrum is the peak for methanol, which reaches its maximum value at about 360 K and then decreases very slowly with increasing temperature. Above 520 K, small amounts of H_2 and CO_2 are observed due to the decomposition of CH_3OH.

Figure 18 shows a TPD spectrum for methanol adsorbed at 298 K on a silica-supported Cu catalyst. The same adsorption conditions were used as for pure silica. Methanol desorbs at 370 K, together with a smaller amount of CH_2O. A well-defined peak for CO_2 is observed at 450 K and two peaks are observed for H_2, one at 380 K and the other at 450 K. The ratio of H_2/CO_2 desorbing at 450 K

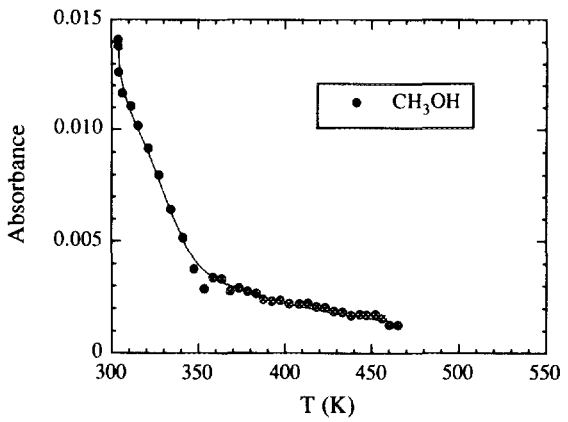

FIG. 11. Temperature dependence of the peak for methanol adsorbed on SiO_2 (3003 cm^{-1}) during the TPD experiment shown in Fig. 10.

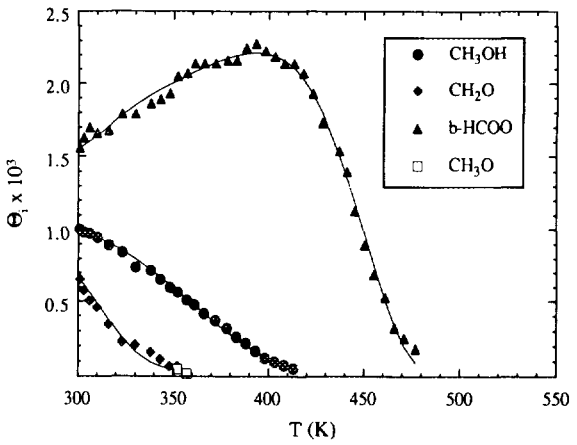

FIG. 13. Temperature dependence of the Cu surface coverages for methanol (2951 cm^{-1}, CH_3O (2822 cm^{-1}), CH_2O (1722 cm^{-1}), and bidentate HCOO (1351 cm^{-1}) during the TPD experiment shown in Fig. 12. Surface coverage for each species is determined from the observed infrared absorbance by using the relationship $\theta_i = A_i/43.5$, where A_i is the absorbance and θ_i is the Cu coverage of species i, respectively. The solid curves represent the best fit to the data based on the model given by Eqs. [1]–[3].

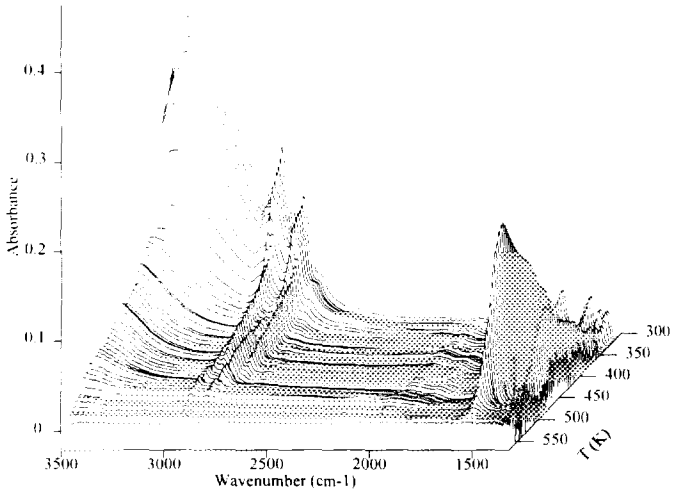

FIG. 14. Infrared spectra obtained during temperature-programmed desorption of methanol from oxidized Cu/SiO_2. Cu/SiO_2 is first exposed to 1% methanol in Ar at 303 K for 10 min, purged in Ar at 303 K for 26 min, and then continuously purged in Ar as the temperature is increased at 5 K/min from 303 to 568 K. Spectra are recorded at 1 min intervals. The spectrum of oxidized Cu/SiO_2 recorded at the same temperature in Ar has been subtracted from each spectrum.

is 0.5 ± 0.04, strongly suggesting that both products arise from the decomposition of HCOO species on the Cu surface. About half of the initially adsorbed CH_3OH desorbs as CH_3OH. From the relative peak areas it is determined that 12% of the CH_3OH not desorbing as CH_3OH undergoes dehydrogenation to form CH_2O, and the remaining 88% decomposes to H_2 and CO_2. Preoxidation of Cu/SiO_2 has no effect on the position of the TPD peaks but the amount of methanol adsorbed decreases by about 9%. The fraction of the adsorbed CH_3OH not desorbing as CH_3OH that undergoes dehydrogenation to CH_2O decreases to 7%, the remainder undergoing decomposition to form H_2 and CO_2.

DISCUSSION

The infrared spectra presented in Figs. 1 and 3 show that methanol adsorbs on the surface of silica as CH_3OH. Molecular CH_3OH is very likely held by hydrogen bonding with Si–OH groups on the surface of the silica. As discussed above, the absence of any $Si–OCH_3$ species is consistent with the published literature. The presence of only physisorbed CH_3OH on SiO_2 is supported, as well, by the observation that all of the features associated with adsorbed methanol disappear at the same rate upon flushing of the sample with Ar (see Fig. 7). A similar pattern is seen during temperature-programmed desorption (see Fig. 11) and analysis of the gas phase during such experiments reveals that methanol is the principal species desorbing from the surface of silica. The appearance of small amounts of CO_2 and H_2 in the desorption products for temperatures of >520 K suggests that CH_3OH undergoes decomposition above 520 K. Since this process was not investigated in detail, nothing can be said about the decomposition pathway of CH_3OH on SiO_2.

Figure 8 shows that the exposure of reduced Cu/SiO_2 to CH_3OH at 303 K results in the concurrent appearance of adsorbed CH_3OH and HCOO. A small amount of CH_2O is also seen, but there is no evidence for CH_3O. The presence of HCOO groups upon exposure of reduced Cu/SiO_2 to methanol has been previously reported by Millar *et al.* (8). However, these authors did not report seeing any evidence for either CH_3OH or CH_2O associated with Cu. In all likelihood this was because the spectrum of CH_3OH adsorbed on SiO_2 was not subtracted from the

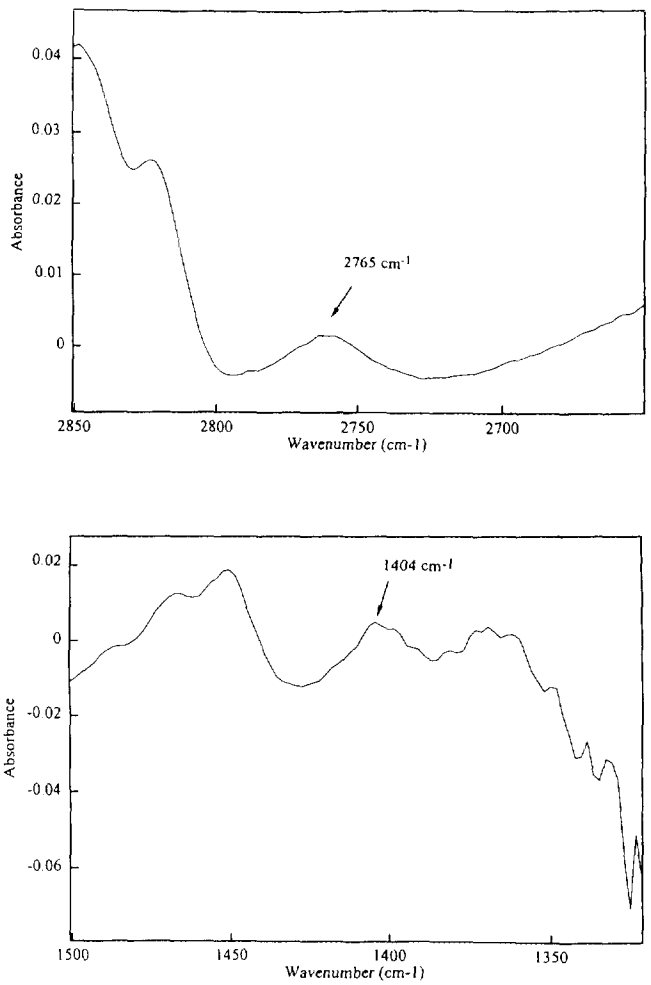

FIG. 15. Blowup of the infrared spectrum recorded 308 K during the temperature-programmed decomposition of methanol adsorbed on oxidized Cu/SiO_2. The bands at 2765 and 1404 cm^{-1} are assigned to $CH_2(O)_2$.

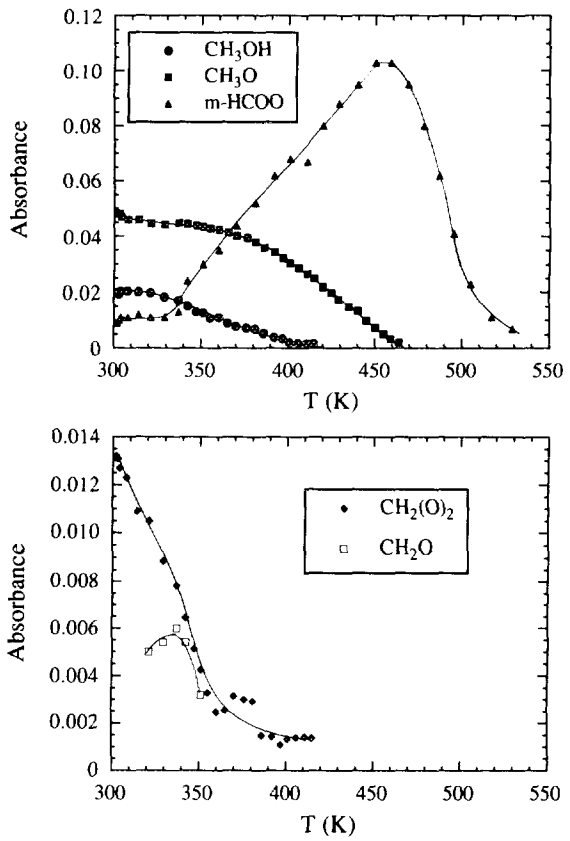

FIG. 16. Temperature dependence of the peaks for methanol (2953 cm^{-1}), CH_3O (2824 cm^{-1}), CH_2O (1718 cm^{-1}), $CH_2(O)_2$ (2765 cm^{-1}), and monodentate HCOO (1592 cm^{-1}) during the TPD experiment shown in Fig. 14.

spectrum of CH_3OH adsorbed on Cu/SiO_2, as was done in the present study.

The TPD spectrum presented in Fig. 18 clearly demonstrates that about half of the CH_3OH adsorbed on reduced

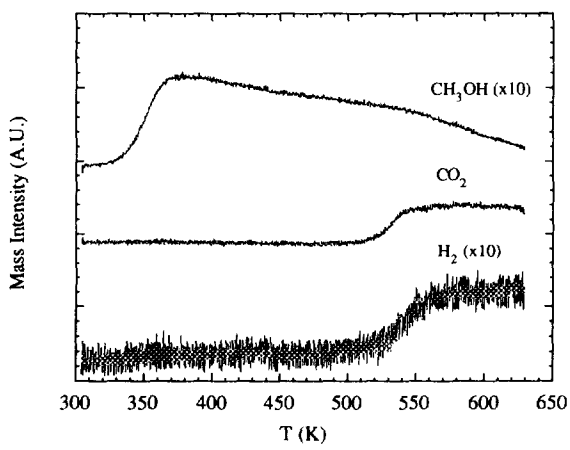

FIG. 17. TPD spectrum obtained after exposure of SiO_2 to 1% methanol for 5 min at 298 K. The heating rate is 10 K/min.

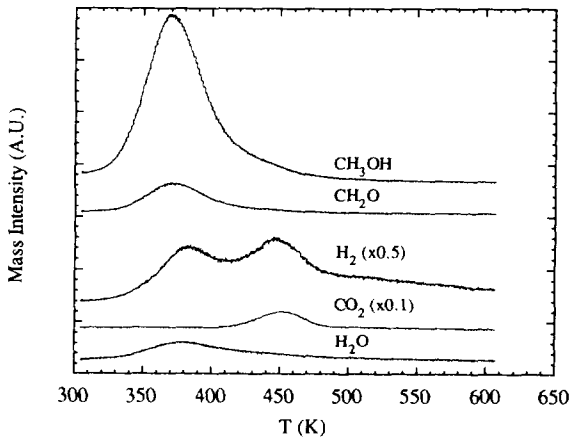

FIG. 18. TPD spectrum obtained after exposure of reduced Cu/SiO_2 to 1% methanol for 5 min at 298 K. The heating rate is 10 K/min.

Cu desorbs as CH_3OH, whereas the other half decomposes to produce a small amount of CH_2O and larger quantities of CO_2 and H_2. The 1 : 2 ratio of the latter two products indicates that CO_2 and H_2 are produced via the decomposition of HCOO species. The infrared spectra taken during temperature-programmed desorption (Figs. 12 and 14) are consistent with the TPD spectra. From the slopes of the curves of CH_2O and HCOO absorbance versus temperature shown in Figs. 13 and 16, it is evident that the maximum rate of disappearance of HCOO from the surface occurs at about 440 K. This temperature is close to the value of 450 K, which is the temperature at which the rate of HCOO decomposition to H_2 and CO_2 reaches a maximum during TPD. The temperature at which the rate of disappearance of CH_2O from the catalyst surface reaches a maximum is 340 K. This is to be compared with the peak maximum for CH_2O desorption observed during TPD, which is 370 K.

The cumulative evidence suggests that the decomposition of CH_3OH over reduced Cu/SiO_2 proceeds via the following reaction pathway shown in Fig. 19, which is similar to that proposed previously by Wachs and Madix (1) to explain the oxidation of CH_3OH on Cu(110) and by Millar *et al.* (39) to explain the synthesis of CH_3OH from CO_2 and H_2 supported Cu catalysts. The initial stage of CH_3OH decomposition is shown to proceed via loss of the hydrogen atom on the alcohol group to form a CH_3O group. While CH_3O groups could not be observed during exposure of reduced Cu/SiO_2 to CH_3OH at 298 K and could be seen in only very small concentration during temperature-programmed desorption, CH_3OH adsorption at 373 K produced a sharp transient in CH_3O shortly after exposure of the catalyst to CH_3OH. The adsorbed CH_3O species undergo further dehydrogenation to form adsorbed CH_2O. Some of the CH_2O desorbs together with H_2 produced by the dehydrogenation of CH_3O. The remaining adsorbed CH_2O is thought to react with oxygen

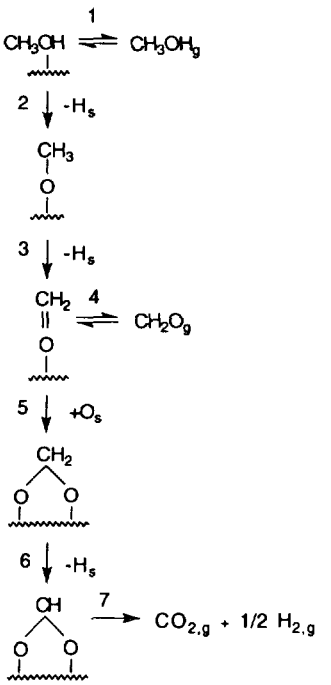

FIG. 19. Proposed mechanism of methanol decomposition over Cu.

present either as adsorbed O atoms on Cu or OH groups near the Cu–SiO_2 border to form $CH_2(O)_2$ groups. While $CH_2(O)_2$ species are not observed during either CH_3OH adsorption or subsequent decomposition over reduced Cu/SiO_2, these species are observable over preoxidized Cu/SiO_2, as discussed below.

Preoxidation of Cu/SiO_2 appears to retard the rates of the dehydrogenation processes occurring during CH_3OH decomposition, so that all of the intermediates appearing in the proposed mechanism (see Fig. 19) can now be observed. Stabilization of CH_3O_s species by adsorbed O_s has been noted previously in studies conducted with both silica-supported Cu and Cu single crystals (1, 8). It has been hypothesized that the stabilization of CH_3O_s occurs through hydrogen bonding between the hydrogen atom of an OH_s group and the oxygen atom of CH_3O_s (8). A similar type of hydrogen bonding has recently been shown to be responsible for the stabilization of OH_s groups at high surface concentrations (40). The presence of O_s is also expected to accelerate the formation of $CH_2(O)_{2,s}$ via addition to CH_2O_s. Stabilization of $CH_2(O)_{2,s}$ to dehydrogenation by the presence of surface O_s or, more likely, OH_s groups is suggested by the slower rise in the formation of $HCOO_s$ groups seen over preoxidized as opposed to reduced Cu/SiO_2. The preferential formation of monodentate, as opposed to bidentate, $HCOO_s$ species on preoxidized Cu might also be attributed to formation of hydrogen bonds with O_s.

The TPD-IR data for methanol decomposition presented in Fig. 13 were simulated to determine the activation energies associated with some of the elementary steps. The reaction mechanism shown in Fig. 19 was used for this purpose. Methanol desorption, reaction 1, and formaldehyde desorption, reaction 4, are assumed to occur reversibly and to be at equilibrium. Since the IR spectra taken during the TPD experiments show that the surface concentrations of CH_3O_s and $CH_2(O)_{2,s}$ are much lower than those of CH_3OH_s, CH_2O_s, and $HCOO_s$, reactions 2 and 3 and reactions 5 and 6 are assumed to occur at equal rates, which is equivalent to saying that the surface concentrations of CH_3O_s and $CH_2(O)_{2,s}$ are at quasi-steady state during a TPD experiment. The surface coverage by adsorbed oxygen is assumed to be constant and is factored into the apparent rate coefficient for reaction 5.

Based on the mechanism presented in Fig. 19 and the assumptions described above, equations can be written for the temperature dependence of the coverages of Cu by CH_3OH_s, CH_2O_s, and $HCOO_s$. These relations are given by

$$\beta\frac{d\theta_1}{dT} = -\left[\frac{F_0}{wC_tK_1^0}\exp(\Delta H_1/RT) + k_2^0\exp(-E_2/RT)\right]\theta_1 \quad [1]$$

$$\beta\frac{d\theta_2}{dT} = k_2^0\exp(-E_2/RT)\theta_1 - \left[\frac{F_0}{wC_tK_4^0}\exp(\Delta H_4/RT) + k_5^0\exp(-E_5/RT)\right]\theta_2 \quad [2]$$

$$\beta\frac{d\theta_3}{dT} = k_5^0\exp(-E_5/RT)\theta_2 - k_7^0\exp(-E_7/RT)\theta_3, \quad [3]$$

where θ_i is the coverage by species i ($i = 1$ is CH_3OH_s, $i = 2$ is CH_2O_s, $i = 3$ is $HCOO_s$), k_j^0 is the preexponential factor for the rate coefficient in reaction j, E_j is the activation energy for reaction j, K_j^0 is the preexponential factor for the equilibrium constant for reaction j, ΔH_j is the enthalpy for reaction j, F_0 is the molar flowrate of the carrier gas, w is the weight of catalyst, C_t is the number of Cu adsorption sites per gram of catalyst, T is temperature, and β is the heating rate.

To simulate the variation in surface coverages of CH_3OHs, CH_2O_s, and $HCOO_s$ with temperature, Eqs. [1]–[3] were solved numerically by using a fourth-order Runga–Kutta algorithm. The initial values for θ_i reported in Fig. 13 were determined from the measured infrared absorbances assuming that the extinction coefficients for CH_2O_s and $HCOO_s$ are equivalent to that for CH_3OH_s. Values of k_j^0, E_j, K_j^0, and ΔH_j were determined by minimizing the sum of square of the errors between the solutions to Eqs. [1]–[3] and the surface coverages determined from the experimental results shown in Fig. 13. The Levenberg–Marquardt optimization algorithm was used for this purpose (41).

TABLE 5

Rate Parameters for Methanol Decomposition

Reaction	k_j^0 (s^{-1})	E_j (kcal/mol)	K_j^0 (atm^{-1})	ΔH_j (kcal/mol)
1	—	—	9.3×10^{10}	−14.5
2	4.7	5.6	—	—
4	—	—	1.1×10^{-3}	−7.7
5	4.9×10^{7}	10.6	—	—
7	5.0×10^{6}	18.8	—	—

Figure 13 shows the extent to which the model represented by Eqs. [1]–[3] fits the experimental observations. It is evident that the agreement between the coverages predicted by the model and those observed experimentally is very close. Values of the rate and equilibrium parameters required to achieve this level of agreement are given in Table 5. Since the quality of the regression was much more sensitive to the magnitudes of the activation energies than those of the preexponential factors, less credence is given to the latter values, but it should be pointed out that a value of K_1^0 less than or equal to 1 did not produce a a good fit. The heat of adsorption for CH_3OH determined from the simulation is 14.5 kcal/mol, in reasonable agreement with the value of 17 kcal/mol reported for Cu(110) (1). By contrast, the estimated heat of adsorption for CH_2O, 7.7 kcal/mol, is a factor of two smaller than that reported for Cu(110) based on an assumed preexponential factor of 10^{13} s^{-1} (1). Of the three elementary processes for which activation barriers have been estimated, reactions 2, 5, and 7, comparison to previous estimates can only be done for reaction 7. The value of 18.8 kcal/mol listed in Table 5 for $HCOO_s$ decomposition to $CO_{2,g}$ and H_s is smaller than the value of 29 kcal/mol reported for the process $HCOO_s \rightarrow CO_{2,g} + H_{2,g}$ occurring on Cu(110) (1). It must be recognized, however, that this process is not an elementary step, and that, consequently, the reported barrier is only an apparent activation energy.

CONCLUSIONS

The present investigation demonstrates that the principal intermediates involved in the decomposition of methanol over silica-supported copper can be observed by infrared spectroscopy. Methanol decomposition is envisioned to proceed via the mechanism presented in Fig. 19. Absorbed methanol first dissociates to produce a methoxy species and adsorbed hydrogen. The methoxy species lose an additional hydrogen atom to form adsorbed formaldehyde, which then reacts with adsorbed oxygen to produce methylenebis(oxy) species. These latter species undergo dehydrogenation to form monodentate or bidentate formate species, which decompose to produce gas-phase carbon dioxide and hydrogen. Simulations of TPD-IR experiments based on the proposed mechanism accurately reproduce the observed variations in the surface concentrations of adsorbed species.

ACKNOWLEDGMENT

This work was supported by the Division of Chemical Sciences, Office of Basic Energy Sciences, U.S. Department of Energy under Contract DE-AC03-76SF00098.

REFERENCES

1. Wachs, I. E., and Madix, R. J., *J. Catal.* **53,** 208 (1978).
2. Sexton, B. A., *Surf. Sci.* **88,** 299 (1979).
3. Sexton, B. A., Hughes, A. E., and Avery, N. R., *Appl. Surf. Sci.* **22/23,** 404 (1985).
4. Barnes, C., Pudney, T., Guo, Q., Bowker, M., *J. Chem. Soc. Faraday Trans.* **86,** 2693 (1990).
5. Ryberg, R., *Phys. Rev. B* **31,** 2545 (1985).
6. Stohr, J., Gland, J. L., Eberhath, W., Outka, D., Madix, R. J., Sette, F., Koestner, R. J., and Doebler, U., *Phys. Rev. Lett.* **51,** 2414 (1983).
7. Fu, S. S., and Somorjai, G. A., *J. Phys. Chem.* **96,** 4542 (1992).
8. Millar, G. J., Rochester, C. H., Waugh, K. C., *J. Chem. Soc. Faraday Trans.* **87,** 2795 (1991).
9. Guerro-Ruiz, A., Rodriguez-Ramos, I., and Fierro, J. L. G., *Appl. Catal.* **72,** 119 (1991).
10. Clarke, D. B., Suzuki, I., and Bell, A. T., *J. Catal.* **142,** 27 (1993).
11. Parris, G. E., and Klier, K., *J. Catal.* **97,** 374 (1986).
12. Hicks, R. F., Kellner, C. S., Savatsky, B. J., Hecker, W. C., and Bell, A. T., *J. Catal.* **71,** 216 (1981).
13. Evans, J. W., Wainwright, M. S., Waugh, K. C., Whan, D. A., *J. Chem. Soc. Faraday Trans. 1* **83** (Faraday Symposium 21), 2193 (1987).
14. Chin, A. A., M.S. Thesis, Department of Chemical Engineering, University of California, Berkeley, CA, 1982.
15. Borrello, E., Zecchina, A., and Morterra, C., *J. Phys. Chem.* **71,** 2938 (1967).
16. Morrow, B. A., *J. Chem. Soc. Faraday Trans.* **87,** 2785 (1974).
17. Falk, M., Whalley, E., *J. Chem. Phys.* **34,** 1554 (1961).
18. Sidorov, A. N., *Zh. Fiz. Khim.* **17,** 145 (1956).
19. Goel, R. G., Prasad, H. S., Bancroft, G. M., and Sham, T. K., *Can. J. Chem.* **54,** 711 (1976).
20. Pouchert, C. J., Ed., "Aldrich Library of FT-IR Spectra Vapor Phase," Vol. 3, The Aldrich Chemical Co., Milwaukee, WI, 1985.
21. Odom, J. D., Wafacz, F. M., Sullivan, J. F., and Durig, J. R., *J. Raman Spec.* **11,** 469 (1981).
22. Nakamoto, K., "Infrared and Raman Spectra of Inorganic and Coordination Compounds," 3rd ed., Wiley, New York, 1978.
23. Millar, G. J., Rochester, C. H., and Waugh, K. C., *J. Chem. Soc. Faraday Trans.* **87,** 2785 (1991).
24. Millar, G. J., Rochester, C. H., Waugh, K. C., *J. Chem. Soc. Faraday Trans.* **87,** 1491 (1991).
25. Millar, G. J., Rochester, C. H., Howe, C., and Waugh, K. C., *Mol. Phys.* **76,** 833 (1991).
26. Anson, C. E., and Powell, D. B., submitted for publication.
27. Chesters, M. A., and McCash, E. M., *Spectrochim. Acta Part A* **43,** 1625, (1987).

28. Sexton, B. A., Hughes, A. E., Avery, N. R., *Surf. Sci.* **155,** 366 (1985).
29. Hayden, B. E., Prince, K., Woodruff, D. P., Bradshaw, A. M., *Surf. Sci.* **133,** 589 (1983).
30. Casey, C. P., Andrews, M. A., Rinz, J. E., *J. Am. Chem. Soc.* **101,** 741 (1979).
31. Sakata, Y., Domen, K., Maruya, K. I., and Onishi, T., *Appl. Surf. Sci.* **35,** 363 (1988–1989).
32. Hayden, B. E., Prince, K., Woodruff, D. P., Bradshaw, A. M., *Phys. Rev. Lett.* **51,** 475 (1983).
33. Davydov, A. A., "Infrared Spectroscopy of Adsorbed Species on the Surface of Transition Metal Oxides," Wiley, Chichester, 1990.
34. Ito, K., and Berstein, H. J., *Can. J. Chem.* **34,** 170 (1956).
35. Jayasooriya, U. P., Anson, C. E., Al-jowder, O., D'Alfonso, G., Stanghellini, P. L., and Rossetti, R., *Surf. Sci.* **294,** 131 (1993).
36. Lavalley, S.-C., Lamotte, J. Busca, G., and Lorenzelli, V., *J. Chem. Soc. Chem. Commun.* 1006 (1985).
37. Kellner, C. S., and Bell, A. T., *J. Catal.* **71,** 296 (1981).
38. Seanor, D. A., and Amberg, C. H., *J. Chem. Phys.* **42,** 2967 (1965).
39. Millar, G. J., Rochester, C. H., and Waugh, K. C., *Catal. Lett.* **14,** 289 (1992).
40. Patrito, E. M., Paredes Olivera, P., and Sellers, H., *Surf. Sci.* **313,** 25 (1994).
41. Press, W. H., Lannery, B. P., Tenkolsy, S. A., and Vetterling, W. T., "Numerical Recipes—The Art of Scientific Computing," Cambrige Univ. Press, New York, 1989.